Measuring the two-photon decay width of intermediate-mass Higgs bosons at a photon-photon collider

T. Ohgaki* and T. Takahashi
Department of Physics, Hiroshima University, 1-3-1 Kagamiyama, Higashi-Hiroshima 739, Japan

I. Watanabe
Akita Junior College, 46-1 Morisawa, Sakura, Shimokitate, Akita 010, Japan†

(Received 7 March 1997)

The feasibility of a measurement of the partial decay width of the intermediate-mass Higgs boson into two photons at a photon-photon collider is studied by a simulation. The QCD radiative correction for quark pair background processes is taken into account for the realistic background estimation. It is found that the two-photon decay width can be measured with the statistical error of 7.6% with about one year of experiment. The impact of the measurement of the two-photon decay width to look for the new physics beyond is demonstrated. [S0556-2821(97)05615-4]

PACS number(s): 14.80.Bn, 13.88.+e

I. INTRODUCTION

The search and the study of Higgs boson, the last missing member of the standard model family, is one of the most important tasks for the current and the future collider experiments at the energy frontier, such as the CERN Large Electron-Positron Collider (LEP II), the Next Linear Collider (NLC), or the CERN Large Hadron Collider (LHC).

The interaction of high energy photons at a photon-photon collider [1–5] provides us with an unique opportunity to study the Higgs boson. The Higgs boson search at the photon-photon collider has been studied by several authors [6–18]. Especially, it has been shown that the search for the intermediate-mass Higgs boson in the mass range $M_W < M_H < 2M_W$ through $\gamma\gamma \to H \to b\bar{b}$ process is complementary to an e^+e^- linear collider [19] or a hadron collider [20–22].

Since two photons do not directly couple to the Higgs boson, but only do through loop diagrams of massive charged particles, any kind of massive charged particles contribute to the two-photon decay width of the Higgs boson if the mass of the loop particle is originated by the Higgs mechanism [23,24]. Figure 1 shows a schematic diagram of the coupling of the Higgs boson with two photons. It is notable that the contribution of a ultra-heavy particle in the two-photon decay width of the Higgs boson has not been suppressed but does keep a sizable constant if its mass is due to the Higgs condensation.

The deviation of the measured two-photon width from its predicted value in the standard model (SM) indicates some additional contributions from unknown particles, and thus it will be a signature of new physics beyond the SM which cannot be provided directly in the ordinary collider experiments. For example, the supersymmetric extensions of the SM have additional charged particles such as scalar fermions, charged Higgs bosons, and charginos. Since the masses of these new particles partly originate from the Higgs bosons, mechanism of the electroweak symmetry breaking, presence of these particles results in a shift of the two-photon decay amplitude of the Higgs boson from its value of the SM. In fact, the minimal extension of the standard model (MSSM) predicts the ratio of the two-photon decay widths $\Gamma(h^0 \to \gamma\gamma, \mathrm{MSSM})/\Gamma(H \to \gamma\gamma, \mathrm{SM})$ as much as 1.2 for the lightest Higgs boson with the mass of 120 GeV [8].

The intermediate-mass Higgs boson in the SM mainly decays into a $b\bar{b}$ pair as is shown in Fig. 2, and the daughter b-flavored hadrons will be easily identified due to their long lifetime; therefore, the $b\bar{b}$ events are the best signals of the intermediate-mass Higgs. The main background may be the continuum $\gamma\gamma \to q\bar{q}$ processes, however, the background events dominantly produced by initial photon collisions in $J_z = \pm 2$ angular momentum state can be suppressed by controlling the polarization of the colliding photon beams. Simultaneously, this control of the beam polarizations causes to enhance the Higgs signals which are only accessible to the

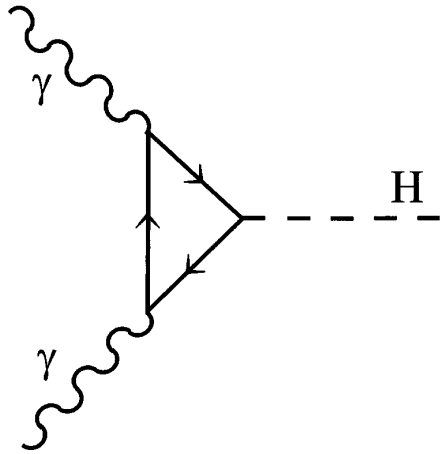

FIG. 1. The coupling of the Higgs boson with two photons generated by a loop of massive charged particle.

*Corresponding author. Electronic address: ohgaki@jlcux1.kek.jp

†The name of the institute has been changed to ''Akita Keizai Hoka University Junior College.''

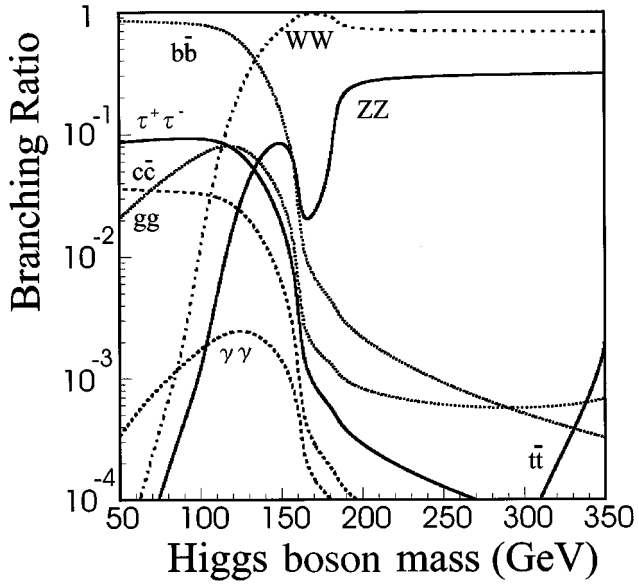

FIG. 2. Branching ratio of the standard model Higgs boson. The top quark mass is assumed to be 176 GeV. Computed by HDECAY [30].

$J=0$ collisions [7,8]. The feasibility of the measurement of the two-photon decay width of Higgs boson in this mass region have been studied using the Monte Carlo simulation by Borden *et al.* [6,8,9].

Recently, several authors reported that the effect of QCD corrections to $\gamma\gamma\rightarrow q\bar{q}$ is large since the helicity suppression which affects the background $q\bar{q}$ events does not work due to a gluon emission. It could be a serious source of backgrounds for the intermediate-mass Higgs, if some of the three-jet events from $J_z=0$ state mimic two-jet events [9,14,15].

In this work we simulate the measurement of the two-photon decay width of the Higgs boson with the mass of 120 GeV at a future photon-photon collider, including the effect of QCD corrections in the manner of Jikia and Tkabladze [15]. To perform a realistic evaluation, the Monte Carlo programs CAIN [25–27], JETSET 7.3 [28] and Japan Linear Collider (JLC-I) detector simulator [29] are applied for a luminosity distribution of a photon-photon collider, hadronizations and selection performances in the detector, respectively. The impact of the measurement for new physics search is discussed with estimated precision.

II. PHOTON-PHOTON COLLISIONS

We first summarize on the photon beam production, beam collision, and luminosity distribution generated by CAIN simulation program [25–27].

As an example of a future linear collider, we adopt the parameters of Japan Linear Collider (JLC) with X-band linear accelerators [29]. In order to hit the mass pole of the Higgs boson at 120 GeV, the center-of-mass energy of the accelerator is tuned to be $\sqrt{s}_{e^+e^-}=150$ GeV. We assume that the spent electrons are bent away by the sweeping magnet so that only scattered photons contribute to the luminosity. The energy of the laser photon is chosen to be 4.18 eV, which results in the maximum photon energy to be roughly 60 GeV. Parameters of the electron and laser beams are shown in Table I. We assume the complete polarizations for both of the electron and laser beams. The combination of the polarizations of the electron P_e and the laser P_L should be $P_eP_L=-1.0$ so that the generated photon spectrum peaks at its maximum energy. With this combination of the electron and the laser beam polarizations, the obtained high energy photon beam is almost completely polarized around the peak energy.

In order to enhance the Higgs boson production and to suppress the background events, the polarizations of the colliding photon beams should be arranged so that the $J_z=0$ collisions dominate. The realistic luminosity distribution of the photon-photon collision is provided by a Monte Carlo simulation program CAIN. CAIN is a comprehensive simulation program of the Compton scatterings and of the beam-beam interactions between laser photons, electrons, and positrons in linear colliders. Figure 3 shows the obtained luminosity distribution of the photon-photon collider at $\sqrt{s}_{e^+e^-}=150$ GeV. The $J_z=0$ and ± 2 components in the luminosity distribution are plotted separately in Fig. 3. As mentioned above, the $J_z=0$ component is dominant in the luminosity distribution and occupies almost 100% around 120 GeV. Figure 4 shows the luminosity distribution in normalized c.m.s. energy z versus rapidity η plane. Here, z and η are defined as

$$z=\sqrt{s}_{\gamma\gamma}/2E_e=\sqrt{w_1w_2}/E_e\,, \tag{1}$$

$$\eta=\ln\sqrt{w_1/w_2}, \tag{2}$$

where $\sqrt{s}_{\gamma\gamma}$ is the $\gamma\gamma$ collision energy, E_e the energy of the electron beam, w_1 and w_2 the energies of left- and right-moving photons, respectively. It is seen from the figure that the Higgs particle of 120 GeV is produced at almost rest, and the low-energy background events like the resolved photon processes are hardly boosted to have completely different topologies from the signal events.

III. EVENT GENERATION AND DETECTOR SIMULATION

A. Signal events

For the intermediate-mass Higgs, the cross section of the process $\gamma\gamma\rightarrow H\rightarrow b\bar{b}$ near the mass pole can be described by the Breit-Wigner approximation:

$$\sigma_{\gamma\gamma\rightarrow H\rightarrow b\bar{b}}=8\pi\,\frac{\Gamma(H\rightarrow\gamma\gamma)\Gamma(H\rightarrow b\bar{b})}{(s_{\gamma\gamma}-M_H^2)^2+M_H^2\Gamma_H^2}\,(1+\lambda_1\lambda_2), \tag{3}$$

where M_H is the Higgs boson mass, $\Gamma(H\rightarrow\gamma\gamma)$ and $\Gamma(H\rightarrow bb)$ the decay widths of the Higgs boson into two photons and b quark pair, Γ_H the total decay width, λ_1 and λ_2 the initial photon helicities, respectively.

The total number of produced Higgs bosons is estimated by convoluting the differential luminosity distribution calculated by CAIN with Eq. (3). The effective cross section $\sigma^{\rm eff}_{|\cos\theta|<0.95}$ obtained by the convolution of differential luminosity distribution with Eq. (3) is given in Table II. A kinematical cut $|\cos\theta|<0.95$ for the scattered angle θ of b and

TABLE I. Parameters of the photon-photon collider based on JLC for $M_H = 120$ GeV.

Electron beam parameters			
Number of electrons per bunch	N_e	0.63×10^{10}	
Number of bunches per pulse	m_b	85	
Repetition rate	$f_{\rm rep}$	150	Hz
Normalized emittance	$\gamma\epsilon_{x,e}$	3.3×10^{-6}	m
	$\gamma\epsilon_{y,e}$	4.8×10^{-8}	m
R.m.s. bunch length	$\sigma_{z,e}$	90	μm
Beta functions at I.P.	$\beta^*_{x,e}$	0.30	mm
	$\beta^*_{y,e}$	10.0	mm
Beam size at I.P. without conversion	$\sigma^*_{x,e}$	82	nm
	$\sigma^*_{y,e}$	57	nm
Beta functions at C.P.	$\beta^{CP}_{x,e}$	0.33	m
	$\beta^{CP}_{y,e}$	20	mm
Beam size at C.P.	$\sigma^{CP}_{x,e}$	2.7	μm
	$\sigma^{CP}_{y,e}$	81	nm
Laser beam parameters			
Wavelength	λ_L	0.297	μm
Photon energy	$\hbar\omega_L$	4.18	eV
R.m.s. pulse length	$\sigma_{z,L}$	300	μm (1 ps)
Laser beam size at C.P.	$\sigma^{CP}_{x,L}$	5	μm
	$\sigma^{CP}_{y,L}$	5	μm
Number of laser photons in a pulse	N_L	1.1×10^{19}	
Energy per pulse	$\hbar\omega_L N_L$	7	Joule
Laser peak power (effective rectangular pulse)	P_L	2.0	TW
Maximum electric field (Gaussian peak)	$\mathcal{E}_{L,\max}$	2.2×10^{12}	V/m
Nonlinear QED parameter at Gaussian peak	$\xi_{\rm peak}$	0.20	
Photon beam			
Number of photons per electron bunch	N_γ	0.41×10^{10}	
Beam size at I.P.	$\sigma^*_{x,\gamma}$	107	nm
	$\sigma^*_{y,\gamma}$	89	nm
$\gamma\gamma$ luminosity	$\mathcal{L}_{\gamma\gamma}$	3.4×10^{32}	$\mathrm{cm}^{-2}\,\mathrm{s}^{-1}$
Distance between C.P. to I.P.	L	1.0	cm

$b\bar{b}$ quarks in the center-of-mass system of the colliding photons is imposed. Throughout our analyses we adopt the quark masses of $m_b = 4.3$ GeV, $m_c = 1.3$ GeV, and $m_t = 176$ GeV. The branching ratios $B(H\to b\bar{b})$ and $B(H\to\gamma\gamma)$ in SM are 64.3% and 0.243%, respectively, which are computed by the HDECAY program [30]. The number of events of the $b\bar{b}$ pairs from Higgs boson decay will be 5,080 for an integrated luminosity of 10 fb^{-1} which roughly corresponds to a one-year run.

For the further analyses of detector acceptance, four-momenta of b and $\bar{b}$ from Higgs boson decay are generated by BASES and SPRING [31]. Subsequent hadronizations of quarks are simulated by the parton shower picture with JETSET 7.3 [28].

B. Background events

The $\gamma\gamma\to q\bar{q}$ background events are generated in a similar way as in the Higgs production, except that the production amplitudes are calculated by HELAS [32], and except that only the events with $\sqrt{s}_{\gamma\gamma} > 75$ GeV are generated. The shapes of three-jet events are reproduced by a parton shower treatment of $q\bar{q}$ evolution by JETSET 7.3, and the QCD corrections of the soft gluon emission, hard gluon emission, and virtual correction to the cross section normalization are taken into account in the manner of Jikia and Tkabladze [15].

The effective cross sections and the number of the generated events of the background processes with and without the QCD corrections are also listed in Table II. In this table, $\gamma\gamma\to q\bar{q}(g)$ indicates the process $\gamma\gamma\to q\bar{q}$ taking account of the QCD corrections. Figure 5 shows the effective cross sections. From this figure, one finds that the QCD correction is drastically large at the maximum collision energy, where the tree $q\bar{q}$ production in $J_z = 0$ mode is hardly suppressed by the helicity conservation law. The effective cross section of $\gamma\gamma\to c\bar{c}$ is larger than that of $\gamma\gamma\to b\bar{b}$ due to the large electric charge of the quark.

In Table II, we also listed the processes of $\gamma\gamma\to H\to c\bar{c}$ and $\gamma\gamma\to H\to gg$ as backgrounds. The branching ratios of $B(H\to c\bar{c})$ and $B(H\to gg)$ are set to be 2.67% and 8.03%, respectively [30].

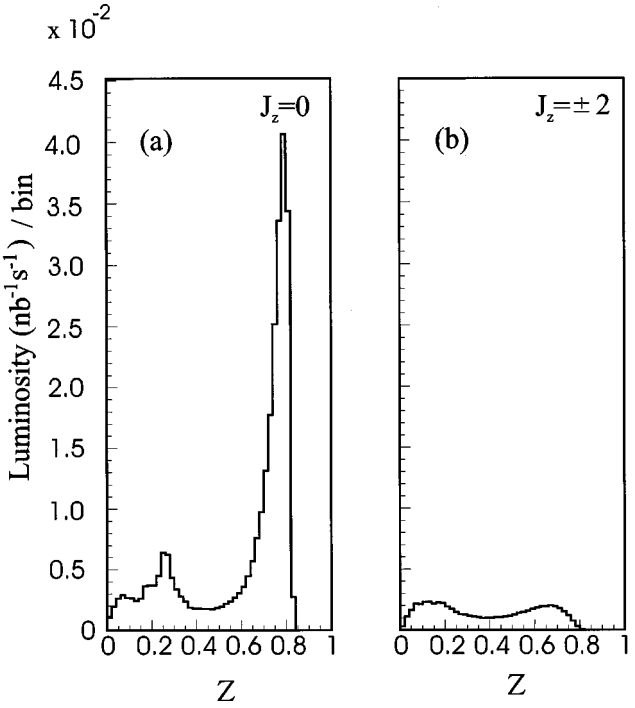

FIG. 3. The polarized luminosity distributions of a photon-photon collider at $\sqrt{s}_{e+e-}=150$ GeV with $P_L P_e=-1.0$. The bin size is 0.02. (a) $J_z=0$. (b) $J_z=\pm 2$.

C. Detector simulation

In order to demonstrate the identification of the Higgs events at a photon-photon collider, we used the JLC detector simulation program which smears the kinematics of the final-state particles according to the JLC-I detector resolution [29]. The performance parameters of the JLC-I detector can be found in Table III. The main components used in this simulator are the vertex detector, central drift chamber, and calorimeters. The b-quark tagging by the vertex detector is crucial in this analysis. A CCD detector is assumed in the current JLC-I design, and its resolution of the impact parameter is

$$\sigma_d^2=11.4^2+(28.8/p)^2/\sin^3\theta(\mu\mathrm{m}^2), \tag{4}$$

where p is the momentum of the charged particle in GeV, θ is the scattering angle.

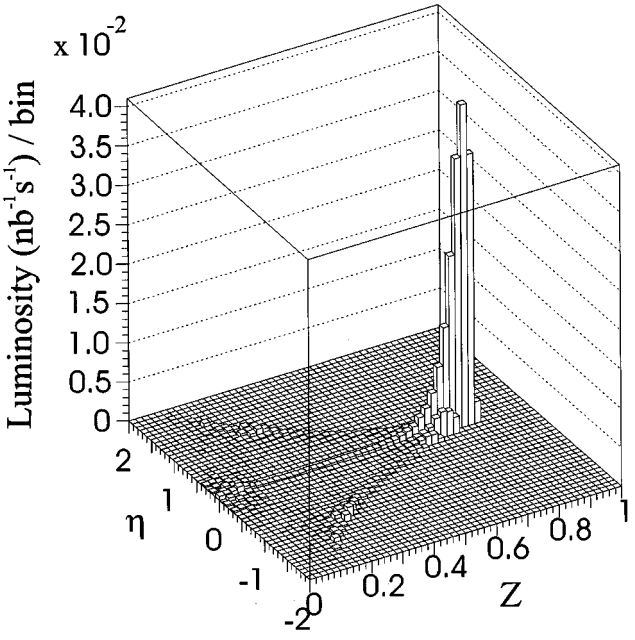

FIG. 4. The luminosity distribution of a photon-photon collider at $\sqrt{s}_{e+e-}=150$ GeV with $P_L P_e=-1.0$ in the z-η plane. The vertical axis is $d^2L_{\gamma\gamma}/dz\,d\eta$ in units of $\mathrm{nb}^{-1}\,\mathrm{s}^{-1}$/bin. The bin size is 0.02×0.08.

TABLE II. Effective cross sections and generated events at a photon-photon collider. The continuum backgrounds are generated as $\sqrt{s}_{\gamma\gamma}>75$ GeV.

	$\sigma^{\mathrm{eff}}_{\lvert\cos\theta\rvert<0.95}$ (pb)	Number of events ($10\ \mathrm{fb}^{-1}$)	Number of simulated events
Signal events			
$\gamma\gamma\to H\to b\bar{b}$	0.508	5080	10000
Backgrounds			
$\gamma\gamma\to H\to c\bar{c}$	0.0210	210	10000
$\gamma\gamma\to H\to gg$	0.0633	633	10000
$\gamma\gamma\to b\bar{b}$	0.502	5020	10000
$\gamma\gamma\to c\bar{c}$	7.19	71900	50000
$\gamma\gamma\to b\bar{b}(g)$	0.727	7270	10000
$\gamma\gamma\to c\bar{c}(g)$	15.1	151000	50000

IV. EVENT ANALYSIS

The analysis requires the reconstruction of the two-jet final states from Higgs boson decay. To identify the $b\bar{b}$ final states from Higgs bosons, we introduce some b-tagging requirements.

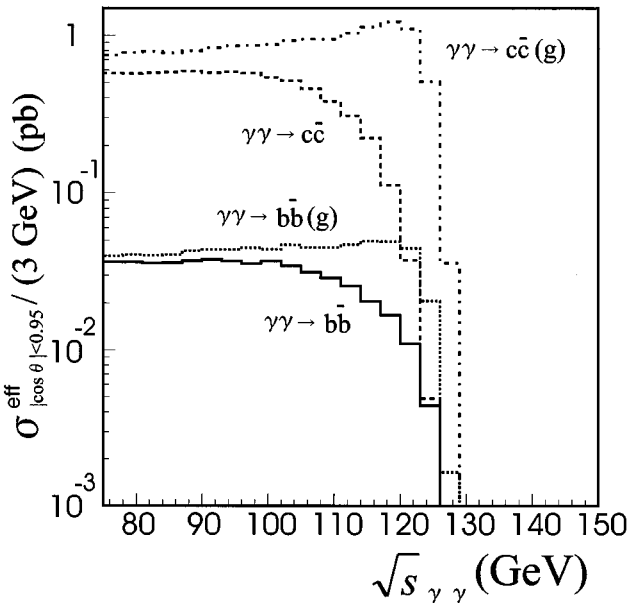

FIG. 5. The collision energy distributions of the effective cross sections at a photon-photon collider. The solid line corresponds to the tree-level $\gamma\gamma\to b\bar{b}$, dashed line to tree-level $\gamma\gamma\to c\bar{c}$, dotted line to $\gamma\gamma\to b\bar{b}$ with QCD corrections and dash-dotted line to $\gamma\gamma\to c\bar{c}$ with QCD corrections. The bin size is 3 GeV.

TABLE III. Performance parameters of the JLC-I detector. The units of energies and momenta are in GeV.

Vertex detector (VTX)	
Position resolution	$\sigma = 7.2\ \mu$m
Impact parameter resolution	$\sigma_d^2 = 11.4^2 + (28.8/p)^2/\sin^3\theta\ (\mu\text{m}^2)$
Central drift chamber (CDC)	
Position resolution	$\sigma_x = 100\ \mu$m, $\sigma_y = 2$ mm
Momentum resolution	$\sigma_{Pt}/Pt = 1.1\times10^{-4} Pt \oplus 0.1\%$
	$\sigma_{Pt}/Pt = 5\times10^{-5} Pt \oplus 0.1\%$
	(with vertex constraint)
Electromagnetic calorimeter (EM)	
Energy resolution	$\sigma_E/E = 15\%/\sqrt{E} \oplus 1\%$
Hadron calorimeter (HAD)	
Energy resolution	$\sigma_E/E = 40\%/\sqrt{E} \oplus 2\%$
Magnetic field	2.0 T

First of all, well reconstructed tracks and clusters in calorimeters are selected from the generated events by the Monte Carlo simulation, and only these tracks and clusters are used in the further analysis. A ''good track'' is required $|\cos\theta| < 0.95$, $P_t > 0.1$ GeV and CDC-VTX track matching. A ''good cluster'' is defined as $E > 0.1$ GeV and $|\cos\theta| < 0.99$.

The number of good tracks is required to be greater than 10 to choose multihadron events, and then two-jet events are selected by JADE clustering algorithm [33] with $y_{\text{cut}} = 0.02$. A cut of $|\cos\theta_{\text{jet}}| < 0.7$, where θ_{jet} is the scattering angle of the jet, is applied to make sure that the events are well contained in the detector volume and to increase the ratio of signal events to backgrounds.

A $b(\bar{b})$ jet is selected by requiring that five or more tracks which have the normalized impact parameter $d/\sigma_d > 2.5$ and $d < 1.0$ mm are in each jet, where d is the impact parameter. Only the events in which that both of the two jets are tagged as b jets are regarded to be the $b\bar{b}$ events to improve the reject probability of the charmed events. The resulting number of the tagged events are summarized in Table IV.

V. RESULTS

To show the effect of QCD radiative corrections to the background processes explicitly, the distribution of the selected events against the reconstructed two-jet invariant mass

TABLE IV. The number of $b\bar{b}$ tagged events with 10 fb^{-1}.

	Events
Signal events	
$H \to b\bar{b}$	582
Backgrounds	
$H \to c\bar{c}$	7.85
$H \to gg$	1.58
$\gamma\gamma \to b\bar{b}$	185
$\gamma\gamma \to c\bar{c}$	715
$\gamma\gamma \to b\bar{b}(g)$	278
$\gamma\gamma \to c\bar{c}(g)$	1320

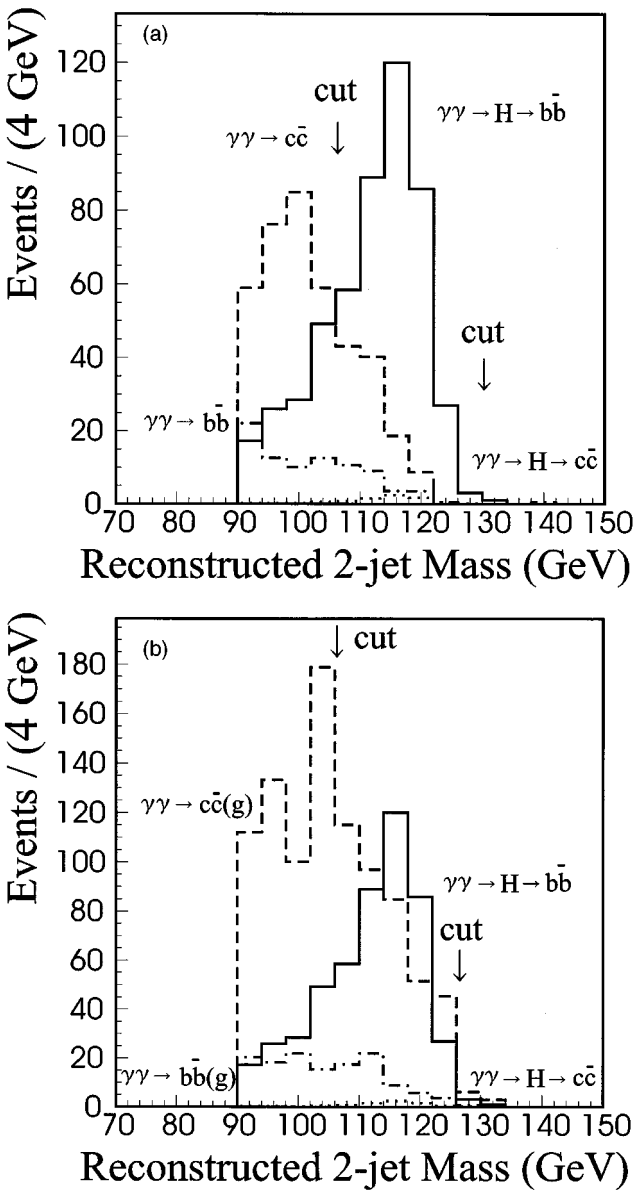

FIG. 6. The reconstructed invariant mass distributions of two-jet events with applying the b-tagging requirements. An integrated luminosity of 10 fb^{-1} and standard model branching fractions for the Higgs boson are assumed. (a) The background events are evaluated in the tree-level. (b) The effect of QCD corrections to background cross sections is taken into account.

M_{jj} at the tree-level and with the QCD corrections are displayed in Fig. 6, separately. In order to enhance the signal, a cut of the invariant mass is tuned in a way that the statistical significance of the signal over backgrounds, $(N_{\text{obs}} - \langle N_{\text{bg}}\rangle)/\sqrt{N_{\text{obs}}}$, is maximized, where N_{obs} is the number of observed events and $\langle N_{\text{bg}}\rangle$ is the number of expected background events. As a results, events in the two-jet mass ranges $106\ \text{GeV} < M_{jj} < 130\ \text{GeV}$ and $106\ \text{GeV} < M_{jj} < 126\ \text{GeV}$ are adopted for the tree-level and QCD corrected evaluations of the backgrounds, respectively. Tables V and VI list the number of events in the invariant mass range, which are the final candidate events as the $\gamma\gamma \to H \to b\bar{b}$. The numbers of estimated signal and background are 383 and 146 from the tree-level computation, while 380 and 459 with the QCD corrections, respectively. Most of the backgrounds are from

TABLE V. The number of the accepted events as candidates of $\gamma\gamma \to H \to b\bar{b}$, selection efficiencies and b-tagging efficiencies in each processes. The tree-level backgrounds are assumed. The invariant mass range $106\ \text{GeV} < M_{jj} < 130\ \text{GeV}$ is adopted.

	Events	ε_{sel} (%)	ε_{tag} (%)
Signal events			
$\gamma\gamma \to H \to b\bar{b}$	383	7.54	64.4
Backgrounds			
$\gamma\gamma \to H \to c\bar{c}$	6.79	3.23	20.3
$\gamma\gamma \to H \to gg$	1.46	0.230	5.82
$\gamma\gamma \to b\bar{b}$	27.1	0.540	77.1
$\gamma\gamma \to c\bar{c}$	111	0.154	15.1
Signal to background at tree level	383/146		

$\gamma\gamma \to c\bar{c}(g)$ process. The selection efficiencies in the above invariant mass ranges,

$$\varepsilon_{\text{sel}} = \frac{\text{No. of selected events}}{\text{No. of generated events}} \tag{5}$$

are listed in Tables V and VI for each case. The $b\bar{b}$-tagging efficiency in the accepted invariant mass range defined as

$$\varepsilon_{\text{tag}} = \frac{\text{No. of selected events}}{\text{No. of two-jet events in the mass range}} \tag{6}$$

is also found in Tables V and VI.

The two-photon decay width of the Higgs boson is proportional to the event rates of the Higgs signal. The statistical error of the number of signal events $\sqrt{N_{\text{obs}}}/(N_{\text{obs}} - \langle N_{\text{bg}} \rangle)$ directly corresponds to the statistical error of the measurement of the two-photon decay width, while the other origins of the errors such as the background subtraction, luminosity distribution, etc., influence the systematic error. Table VII lists the statistical errors of two-photon decay width of the Higgs boson. The two-photon decay width of the SM Higgs boson at $M_H = 120\ \text{GeV}$, in the estimate with the QCD corrections to $\gamma\gamma \to q\bar{q}$ background processes, is 7.6%.

TABLE VI. The number of the accepted events as candidates of $\gamma\gamma \to H \to b\bar{b}$, selection efficiencies and b-tagging efficiencies in each processes. The backgrounds with QCD corrections are assumed. The invariant mass range $106\ \text{GeV} < M_{jj} < 126\ \text{GeV}$ is adopted.

	Events	ε_{sel} (%)	ε_{tag} (%)
Signal events			
$\gamma\gamma \to H \to b\bar{b}$	380	7.48	64.3
Backgrounds			
$\gamma\gamma \to H \to c\bar{c}$	6.65	3.16	20.1
$\gamma\gamma \to H \to gg$	1.46	0.230	5.88
$\gamma\gamma \to b\bar{b}(g)$	57.4	0.790	69.9
$\gamma\gamma \to c\bar{c}(g)$	394	0.260	16.2
Signal to background with QCD corrections	380/459		

TABLE VII. Statistical errors on the measurement of two-photon decay width of SM Higgs boson with the mass of 120 GeV. An integrated luminosity of 10 fb^{-1} is assumed.

$\Delta X/X$	Tree level	QCD correction
$\Gamma(H \to \gamma\gamma)$	6.0%	7.6%

VI. SUMMARY

We have studied the feasibility of the measurement of two-photon decay width of intermediate-mass Higgs boson in the standard model at a photon-photon collider by Monte Carlo simulations of photon-photon collisions, hadronizations, and detector simulation. The QCD radiative corrections to the background process $\gamma\gamma \to q\bar{q}$ are taken into account. The statistical error on the measurement of the two-photon decay width of the Higgs boson with the mass of 120 GeV is 7.6% for the integrated luminosity of 10 fb^{-1}. At the integrated luminosity of 20 fb^{-1}, the ratio of signal to background is improved to be 760/919, and the statistical errors on the two-photon decay width measurement for 120 GeV Higgs boson is 5.4%.

The statistical errors of the two-photon decay width of the intermediate-mass Higgs boson using Monte Carlo simulation by Borden *et al.* [8] are within 5% when the background events at tree-level and the integrated luminosity 20 fb^{-1} are assumed. The statistical errors in our analysis are comparable with their study. In [8], the $b\bar{b}$-tagging efficiency is assumed to be 50% with 5% $c\bar{c}$ contamination, while it is estimated to be 64.4% with 15.1% contamination by the detector simulation in the present study. Since the adopted b-quark tagging algorithm in our analysis is simple one in which the three dimensional impact parameters are computed from the tracking data in the vertex detector, it is expected that the developments of new tagging algorithms and particle identification can be more efficient in separating $H \to b\bar{b}$ events from other backgrounds.

This result shows, for instance, that the photon-photon collider will be sufficient to distinguish the intermediate-mass Higgs boson of SM from the lightest Higgs of MSSM, if the ratio of the two-photon decay widths $\Gamma(h^0 \to \gamma\gamma, \text{MSSM})/\Gamma(H \to \gamma\gamma, \text{SM})$ is as large as 1.2 [8]. It indicates that a photon-photon collider has a great and unique feasibility to look for the new physics beyond SM.

ACKNOWLEDGMENTS

We greatly appreciate Professor I. Endo for useful discussions and encouragement. We would like to thank Professors G. Jikia, J. Kamoshita, T. Kon, Y. Okada, T. Takeshita, T. Tauchi, A. Tkabladze, A. Miyamoto, and K. Yokoya for useful discussions. We thank members of Photon Physics Laboratory at Hiroshima University, and members of Akita Junior College. This work was partly supported by the Grant-in-Aid for Scientific Research from Ministry of Education, Science and Culture of Japan. One of the authors (T. O.) would like to thank the Research Fellowships of the Japan Society for the Promotion of Science for Young Scientists for financial support.

[1] I. F. Ginzburg, G. L. Kotkin, V. G. Serbo, and V. I. Telnov, Pisma Zh. Eksp. Teor. Fiz. **34**, 514 (1981) [JETP Lett. **34**, 491 (1981)].
[2] I. F. Ginzburg, G. L. Kotkin, V. G. Serbo, and V. I. Telnov, Nucl. Instrum. Methods Phys. Res. **205**, 47 (1983); Nucl. Instrum. Methods Phys. Res. A **219**, 5 (1984).
[3] V. I. Telnov, Nucl. Instrum. Methods Phys. Res. A **294**, 72 (1990).
[4] V. I. Telnov, in *Proceedings of the Workshop on Gamma-Gamma Colliders*, Berkeley, CA, 1994, edited by S. Chattopadhyay *et al.* [Nucl. Instrum. Methods Phys. Res. A **355**, 3 (1995)].
[5] Y. Yasui, I. Watanabe, J. Kodaira, and I. Endo, Nucl. Instrum. Methods Phys. Res. A **335**, 385 (1993).
[6] D. L. Borden, D. A. Bauer, and D. O. Caldwell, SLAC Report No. SLAC-PUB-5715, 1992 (unpublished).
[7] J. F. Gunion and H. E. Haber, Phys. Rev. D **48**, 5109 (1993).
[8] D. L. Borden, D. A. Bauer, and D. O. Caldwell, Phys. Rev. D **48**, 4018 (1993).
[9] D. L. Borden, V. A. Khoze, W. J. Stirling, and J. Ohnemus, Phys. Rev. D **50**, 4499 (1994).
[10] M. Baillargeon, G. Bélanger, and F. Boudjema, ENSLAPP Report No. ENSLAPP-A-473/94, 1994 (unpublished).
[11] M. Baillargeon, G. Bélanger, and F. Boudjema, Phys. Rev. D **51**, 4712 (1995).
[12] I. Watanabe, in *Proceedings of INS Workshop on the Physics of e^+e^-, $e^-\gamma$ and $\gamma\gamma$ Collisions at Linear Accelerators*, Tokyo, 1994, edited by Z. Hioki, T. Ishii, and R. Najima (Report No. INS-J-181, 1995), p. 139.
[13] I. Watanabe, in *Proceedings of Workshop on Physics and Experiments with Linear Colliders*, Morioka-Appi, Iwate, Japan, 1995, edited by A. Miyamoto, Y. Fujii, T. Matsui, and S. Iwata (World Scientific, Singapore, 1996), p. 689.
[14] G. Jikia and A. Tkabladze, Nucl. Instrum. Methods Phys. Res. A **355**, 81 (1995).
[15] G. Jikia and A. Tkabladze, Phys. Rev. D **54**, 2030 (1996).
[16] S. Kuhlman *et al.*, the NLC ZDR Design Group and the NLC Physics Working Group, Report No. BNL 52-502, 1996 (unpublished).
[17] G. V. Jikia, Nucl. Phys. **B405**, 24 (1993).
[18] R. Najima, in *Proceedings of Third Meeting on Physics at TeV Energy Scale*, Tsukuba, Japan, KEK, 1989, edited by K. Hidaka and C. S. Lim (KEK Report No. 90-9, Tsukuba, 1990), p. 112.
[19] D. R. T. Jones and S. T. Petcov, Phys. Lett. **84B**, 440 (1979).
[20] J. F. Gunion, G. L. Kane, and J. Wudka, Nucl. Phys. **B299**, 231 (1988).
[21] J. F. Gunion, Phys. Lett. B **261**, 510 (1991).
[22] Z. Kunszt, Z. Trocsanyi, and W. J. Stirling, Phys. Lett. B **271**, 247 (1991).
[23] J. F. Gunion, H. E. Haber, G. L. Kane, and S. Dawson, *The Higgs Hunter's Guide* (Addison-Wesley, Redwood City, CA, 1990).
[24] L. B. Okun, *Leptons and Quarks* (North-Holland, Amsterdam, 1982).
[25] P. Chen, G. Horton-Smith, T. Ohgaki, A. W. Weidemann, and K. Yokoya, Nucl. Instrum. Methods Phys. Res. A **355**, 107 (1995).
[26] T. Ohgaki and T. Takahashi, Nucl. Instrum. Methods Phys. Res. A **373**, 185 (1996).
[27] P. Chen, T. Ohgaki, A. Spitkovsky, T. Takahashi, and K. Yokoya (in preparation).
[28] T. Sjöstrand, Comput. Phys. Commun. **82**, 74 (1994).
[29] ''*JLC-I*,'' KEK Report 92-16, 1992 (unpublished).
[30] M. Spira, in Proceedings of 5th International Workshop on New Computing Techniques in Physics Research: Software Engineering, Neural Nets, Genetic Algorithms, Expert Systems, Symbolic Algebra, Automatic Calculations (AIHENP 96), Lausanne, Switzerland, 1996 (unpublished).
[31] S. Kawabata, Comput. Phys. Commun. **41**, 127 (1986); **88**, 309 (1995).
[32] H. Murayama, I. Watanabe, and K. Hagiwara, KEK Report 91-11, 1992 (unpublished).
[33] JADE Collaboration, W. Bartel *et al.*, Z. Phys. C **26**, 93 (1984).